Enhancement of Power Conversion Efficiency $CuSbSe_2$ Based Dual Heterojunction Thin Film Solar Cell

Hafizur Rahman Alve[1,2‡], Saiful Islam [2], N.K Das [2], Mrinmoy Dey[2]

[1]Institute of Energy, University of Dhaka, Dhaka-1000, Bangladesh

[2]Department of Electrical and Electronic Engineering, Chittagong University of Engineering and Technology, Chattogram- 4349, Bangladesh

(alve8969@gmail.com, u1702098@student.cuet.ac.bd, nipudas@cuet.ac.bd, mrinmoy@cuet.ac.bd))

‡Corresponding Author; Hafizur Rahman Alve, Department of Electrical and Electronic Engineering, Chittagong University of Engineering and Technology, Chattogram- 4349, Bangladesh, Tel: +8801645084581, alve8969@gmail.com

Received: 01.09.2024 Accepted: 28.09.2024

Abstract- In this research work, we show how to develop and simulate Copper Antimony Selenide ($CuSbSe_2$) based thin film solar cell with dual-heterojunction. Copper Antimony Selenide ($CuSbSe_2$) creates a p-n junction with a window layer and another p-p^+ connection with a highly doped back surface Field (BSF) layer, and a dual-heterojunction solar cell structure is produced. Using SCAPS-1D software, which incorporates published experimental physical parameters, the simulation was run. The simulation results show that the PCE of the single heterojunction structure (n-CdS/p-$CuSbSe_2$/Ni) solar cell may reach 27.12 % with V_{oc}=0.738 V, J_{sc}=43.08 mA/cm^2 & FF=85.23 % with the normal level of temperature coefficient (TC). For the dual heterojunction structure (n-CdS/p-$CuSbSe_2$/p^+-CGS/Ni) the results exhibit the best Power Conversion Efficiency (PCE) as high as 46.32 % with V_{oc}=1.053 V, J_{sc}=54.34 mA/cm^2 & FF=80.97 % and a good level of temperature coefficient (TC) is found to be (-0.042 %/◦C).

Keywords: Dual-heterojunction; $CuSbSe_2$; BSF; PCE; Thermal stability.

Nomenclature

Symbol

W (μm)	Thickness	N_t (eV^{-1}cm^{-3})	Peak defect density
ϵ_r	Dielectric Relative Permittivity	N_V (cm^{-3})	Valance Band Effective Density
χ	Electron Affinity	N_C (cm^{-3})	Conduction Band Effective Density
E_g (eV)	Band Gap	N_d (cm^{-3})	Donor Density
V_{oc} (V)	Open Circuit Voltage	N_a (cm^{-3})	Acceptor Density
J_{sc} (mA/cm^2)	Short Circuit Current	μ_e (cm^{-2}/Vs)	Electron Mobility
FF (%)	Fill Factor	μ_h (cm^{-2}/Vs)	Hole Mobility
η (%)	Efficiency	T (K)	Temperature

Acronyms and Abbreviations

BSF	Back Surface Field
CdS	Cadmium Sulfide
$CuSbSe_2$	Copper Antimony Selenide
CGS	Copper Gallium Selenide
Ni	Nickel
PCE	Power Conversion Efficiency
Ti	Titanium

1. Introduction

The ongoing years have seen a ton of interest in slender film sun powered cells as per best proficiency safeguards because of its expected use in adaptable photovoltaic innovation [1]. The transformation productivity of sun powered cells utilizing CdTe and Cu(In,Ga)Se_2 (CIGS) as engrossing layers has proactively been reached at 22% [2] and 23% [3]. Temperature evaporation has a significant influence on the output power of solar systems in thin-film solar cells [4, 5]. The structural and optical features indicate that the produced CdTe films can serve as an appropriate absorber layer for thin film-based solar cells [6, 7, 8]. However, the advanced and use of such solar cells have been severely constrained by the lack of In, the poisonousness of Cd, and the significant expense of Ga. Making another material for meager film sun oriented cells considering these factors is required. Numerous possible absorber materials have been investigated to far, including Cu_2ZnSnS_4 [9], $CuSbS_2$ [10, 11] and $CuSbSe_2$ [12]. $CuSbSe_2$ is a strong contender for use in thin-film solar cells because it has an acceptable band gap of around 1.1 eV. It is inexpensive, low in poisonousness, and plentiful in the world's outside. $CuSbSe_2$ also has a high absorption coefficient at short wavelengths (> 10^4 cm^{-1}) [[13]. The $CuSbSe_2$ sun powered cell has a hypothetical transformation proficiency of around 30%, which is close to the utmost possibility, according to the studies done by Wang et al. [14]. $CuSbSe_2$ ternary films have been prepared using a variety of techniques up to this point. For instance, utilising electro deposition and a quick annealing procedure, Tang et al. created $CuSbSe_2$ film [15]. A new and simple hot injection technique was adopted by Hsiang et al. [16]. The Sb/Cu metal precursors were created by Colombara et al. by sequential evaporation and subsequent annealing in a quartz cylindrical heater with selenium powder [17]. Jiangxue et al. spin-coated the Cu-Sb-Se precursor solution onto the glass, then heated the samples in a furnace to anneal them. With the exception of substituting the Cu-Sb-Se precursor solution with a precursor combination of Sb_2Se_3 and Cu_2S, Yang et al. employed the identical process as Jiangxue's group [18]. Wang et al. used close-spaced sublimation at a predefined temperature to evaporate the Sb_2Se_3 before creating the $CuSbSe_2$ films [19]. Initially, they pre-sputtered a Cu layer. Given $CuSbSe_2$'s favorable electrical and optical properties and its readily available, affordable, and non-toxic component elements, it appears to be a promising protection material for thin-film solar cells. Nevertheless, a thorough investigation of the essential features of $CuSbSe_2$, including its defect physics, material, optical, and electrical properties all of which are crucial for photovoltaic applications has not yet been conducted. Based on the Shockley–Queisser detailed-balance theory, a structure of dual heterojunction solar cell can have a maximum efficiency of between 42% and 46% [20, 21]. A three-terminal dual- heterojunction bipolar transistor solar cell with a theoretical efficiency potential of around 54.7% has been claimed by Marti et al. [22]. In this investigation, a thin-film solar cell based on copper antimony selenide ($CuSbSe_2$) is designed and simulated to achieve high efficiency. Solar cells based on copper antimony selenide ($CuSbSe_2$) have been extensively studied in the past, the cell structure of *n*-ZnSe/p-$CuSbSe_2$/p^+-CGS with V_{oc}=0.935 V, J_{sc}=58.943 mA/cm^2, FF=79.46 %, and A PCE of 43.77 was found to be the most recent top result [23].

The primary goal of this study is to model a Copper Antimony Selenide ($CuSbSe_2$)-based thin film solar cell with a stable cell structure and more optimal performance. This novelty of this research paper introduces a new dual heterojunction cell construction. The dual-heterojunction approach involves the absorber layer forming a p-n junction with a window layer and another p-p^+ connection with a highly doped back surface Field (BSF) layer. As a result, a dual heterojunction is formed. In order to determine the ideal window layer structure, we examine the performance of CdS window layers with different thicknesses and doping concentration. As a back surface field (BSF) layer, we used copper gallium selenide (CGS) and we assessed the performance according to thickness and doping concentration. Finally, we built dual-heterojunction solar cell with cell structure n-CdS/p-$CuSbSe_2$/p^+-CGS/Ni and the best power conversion efficiency (PCE) was 46.32%.

2. Modeling and Simulation

The simulation was conducted with experimental physical parameters using SCAPS-1D software. SCAPS-1D uses Poisson's equation, the drift-diffusion equations, continuity equations for electrons and holes in one dimension and uses numerical algorithms like the Newton-Raphson Method, Finite Difference Method (FDM), and Gummel's Method to resolve complicated equations that explain the operation of solar cells. Numerical simulations were powered by a single sun with 100 mW/cm^2 of light along with a 1.5G spectrum global air mass (AM). At 300 K, the operational temperature was being measured. There was no consideration of the radiative recombination coefficient, and the optimal values of shunt and series resistance were employed. The bulk layers were assumed to have Gaussian acceptor and donor doping patterns, and interface defects were also analyze.

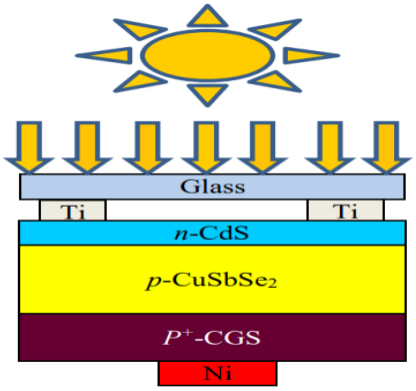

Fig. 1. Proposed structure of $CuSbSe_2$ solar cell

The simulated schematic design of the dual-heterojunction n-CdS/p-$CuSbSe_2$/p^+-CGS/Ni cell is shown in "Figure 1". Nickel (Ni) works as the back contact in this

structure. Incoming sunlight is absorbed by the CGS and $CuSbSe_2$ layers, after it has passed through the CdS layer. $CuSbSe_2$ has an ionization potential of 5.19 eV and an electron affinity of 4.11 eV [23], whereas CdS has an ionization potential of 8.7 eV and an electron affinity of 4.4 eV [24, 25]. Because of this, CdS is a good material to use with $CuSbSe_2$ to generate a p-n heterojunction. Furthermore, owing to its 1.66 eV band gap and 3.67 eV electron affinity [26], CGS may create a suitable p-p^+ heterojunction with $CuSbSe_2$. In the presence of the appropriate energy barriers, the holes created by the $CuSbSe_2$ and CGS layers can migrate toward the anode, making it easier for them to reach the cathode. The percentage of the incident power that is converted into electric power, which is indicative of a solar cell's efficiency, may be determined utilizing the formula below:

$$\eta = \frac{V_{OC}\, I_{SC}\, FF}{P_{in}} \qquad (1)$$

Where, P_{in} is the incident solar power (in watts).

Table 1. Electrical parameter of different layers for simulation in SCAPS

Material Properties	CdS [25]	$CuSbSe_2$ [23]	CGS [26, 27, 28]
Thickness (µm)	0.05	0.8	0.2
Dielectric permittivity, ϵ_r	9	15	8.5
Bandgap, E_g (eV)	2.4	1.08	1.66
Electron affinity, χ (eV)	4.4	4.11	3.67
N_c (cm^3)	2.2×10^{18}	9.9×10^{19}	2.2×10^{17}
N_v (cm^3)	1.8×10^{19}	9.9×10^{19}	1.8×10^{18}
μ_h (cm^2/Vs)	25	10	25
μ_e (cm^2/Vs)	100	10	100
N_a (cm^{-3})	0	1×10^{16}	1.0×10^{19}
N_d (cm^{-3})	1×10^{18}	0	0
Distribution	Gaussian	Gaussian	Single
Type of defect	Acceptor	Donor	Donor
N_t [$eV^{-1}cm^{-3}$]	5.642×10^{13}	5.642×10^{12}	1×10^{14}
Reference Energy [eV]	1.350	0.650	0.6

3. Results and Discussion

3.1. CdS Window Layer Effect on Cell Performance

CdS, a well-known window layer with the bandgap of 2.42 eV, is one of the window layers most suited for PV applications. Since it directs the majority of incoming photons onto the absorber, CdS remains unchanged. A variety of processes, among them are chemical bath deposition (CBD) [29], physical vapour deposition (PVD), and chemical vapour deposition (CVD) [30], and close spaced sublimation (CSS) procedures [31], have been used to produce CdS thin films. The conversion efficiency of a slight film sun based cell can be essentially impacted by the thickness of the CdS window layer. In thin film solar cells, the CdS layer is frequently utilised as a window layer to promote effective lower recombination losses and carrier collection. The all out presentation of the sun oriented cell might be influenced in various ways by fluctuating the thickness of the CdS window film. The CdS window film generally has a range of ideal thicknesses that offer the optimum compromise between carrier collecting and light transmission. The thickness is selected to provide the absorber layer with adequate transparency so that incoming light may reach it while yet efficiently absorbing photo generated carriers. Depending on the particular solar cell design, the materials used, and the device architecture, this ideal thickness may change [32].

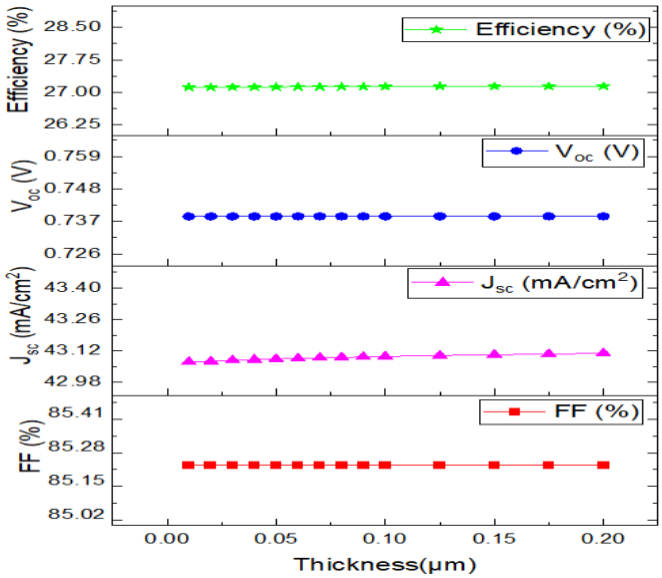

Fig. 2. Thickness variation of CdS

Thickness fluctuation of CdS window layer is seen in "Figure 2" between 0 and 200 nm, we observed almost constant value of V_{oc}, J_{sc} & FF. As a result, efficiency was almost same as 27.13 %. We observed optimize values of thickness at 55 nm.

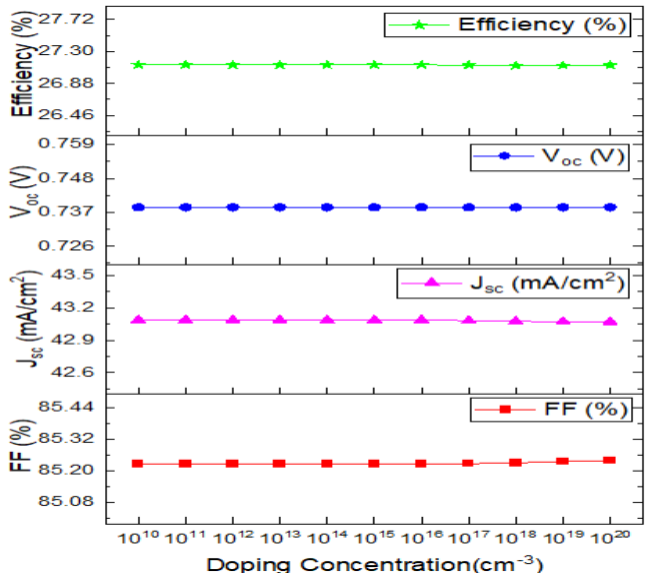

Fig. 3. Doping Concentration variation of CdS

It's vital to keep in mind that ideal doping concentration might vary based on the unique solar cell design, materials

employed, and device architecture when comparing the total doping concentration of CdS window layer [33]. The variation in the CdS window layer doping concentration is demonstrated in "Figure 3" from 10^{10} cm^{-3} to 10^{20} cm^{-3}. We observed almost constant value for the V_{oc} and J_{sc} & FF slightly increased. As a result, the efficiency was almost same value of 27.12 % from 10^{10} cm^{-3} to 10^{16} cm^{-3} then slightly increased.

3.2. Impact of CGS BSF Layer

At solar cell's back surface, BSF layer serves as a barrier to stop carrier recombination. By properly separating the photon generated electrons and holes in an area of high electric field, it decreases the likelihood of them recombining and lengthens their lifespan. The BSF layer aids in maximising the solar cell's total conversion efficiency by reducing carrier recombination [34].

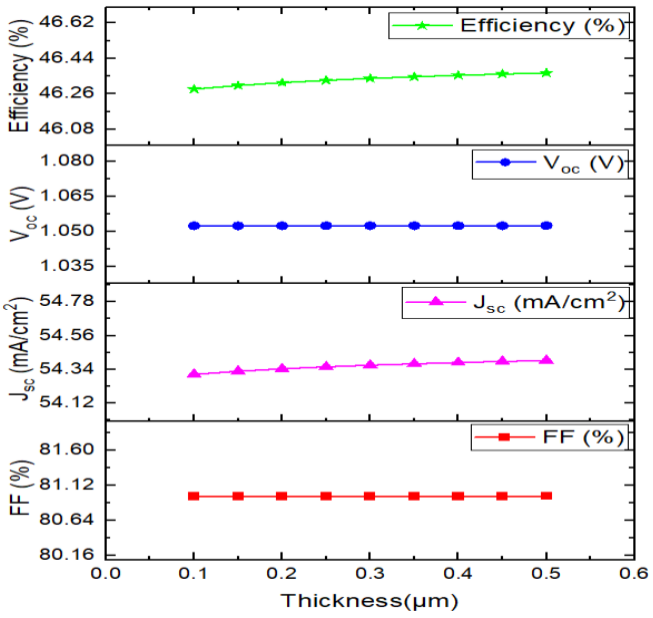

Fig. 4. Thickness variation of CGS

Thickness of CGS BSF layer differs from 100 to 500 nm, as shown in "Figure 4", we observed almost constant value for V_{oc} and FF remain almost constant. On other hand, value of J_{sc} was slightly increased. As a result, the efficiency slightly increased from 46.28 % to 46.37 %. 200 nm was selected for the cell's stable structure and cost-effectiveness. Through the creation of a stronger electric field close to the back surface, the BSF layer improves carrier collecting. This field directs the photon generated carriers towards the direction of contacts, enabling effective extraction. A greater photocurrent results the better carrier collection, which boosts the solar cell's overall performance.

Doping can also influence the bandgap of the CGS BSF layer. It is feasible to adjust the bandgap and electrical structure of CGS by varying doping concentration. As a result, this bandgap engineering can optimize the alignment with the absorber layer's bandgap, allowing for effective light absorption and carrier collection, and potentially boosting the solar cell's conversion efficiency. The fluctuation in the CGS doping concentration is seen in "Figure 5" from 10^{10} cm^{-3} to 10^{20} cm^{-3}, we observed almost constant value of V_{oc}, J_{sc} & FF at 10^{17} cm^{-3}, as a result, the efficiency was almost constant at 46.32%. After increasing the value of doping concentration, efficiency slightly decreased.

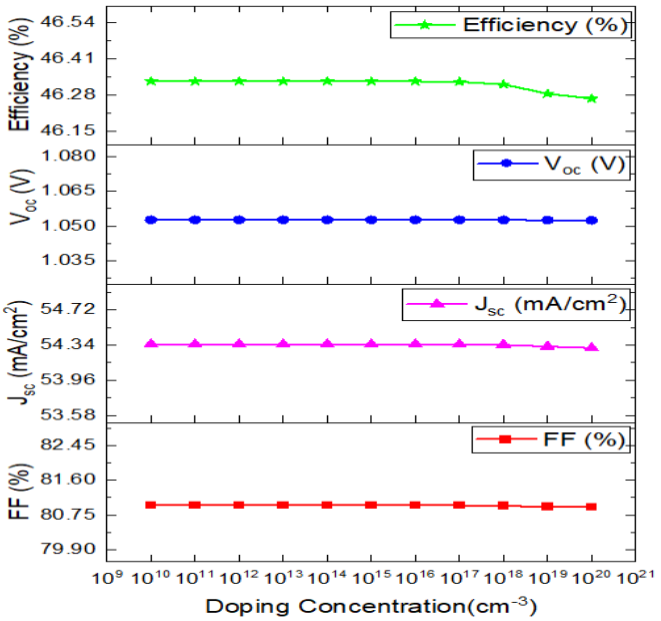

Fig. 5. Doping Concentration Variation of CGS

4. Variation of Defect Density

The performance and efficiency of solar cells are greatly impacted by defect density, making it an important aspect to consider. Reducing fault density is crucial to raising solar cell performance, efficiency, and dependability. Scientists and producers concentrate on methods to lessen imperfections in semiconductor material to create high-grade, high-efficiency solar cells. As a part of our inquiry into the impact of fault density, we have conducted experiments in which the value of imperfection density changed from 10^{10} cm^{-3} to 10^{20} cm^{-3}, while the ideal layer thickness remained same.

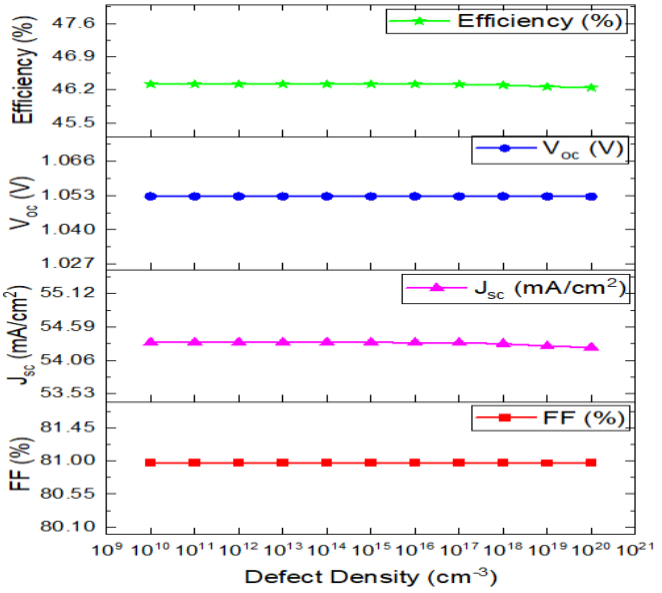

Fig. 6. Variation of Defect Density for $CuSbSe_2$ Solar Cell

"Figure 6" shows the parameter curves for a number of different deficiency densities that were measured. This deterioration in quality may be linked to an increase in the recombination rate that happens with an increase in the defect density. Together, these two factors contribute to an overall rise in the defect density. In contrast, when the fault density is lower than 10^{18} cm^{-3} we saw almost constant values V_{oc}, J_{sc} & FF, as a result, the efficiency was almost constant.

5. Temperature Impact on Cell Structure

The variability of cell parameters is impacted by changes in operating temperature. To investigate the potential of the $CuSbSe_2$ absorber layer, the researchers investigated the thermal stability of the proposed solar cell [14, 35].

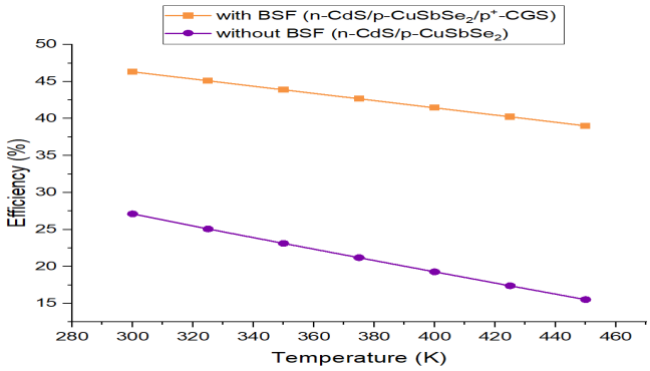

Fig. 7. Effects of operating temperature with and without a BSF layer

The effects of operation temperature on efficiency with and without a BSF layer are depicted in "Figure 7" and the impact of operating temperature on BSF cell structure from 250 K to 500K is shown in "Figure 8". It is seen that the single cell structure without BSF (n-CdS/p-$CuSbSe_2$/Ni) has lower efficiency and the temperature coefficient of (-0.22%/◦C). On other side, dual heterojunction structure (n-CdS/p $CuSbSe_2$/p^+-CGS/Ni) has higher efficiency and temperature coefficient of (-0.042%/◦C) which denotes a good level of temperature stability.

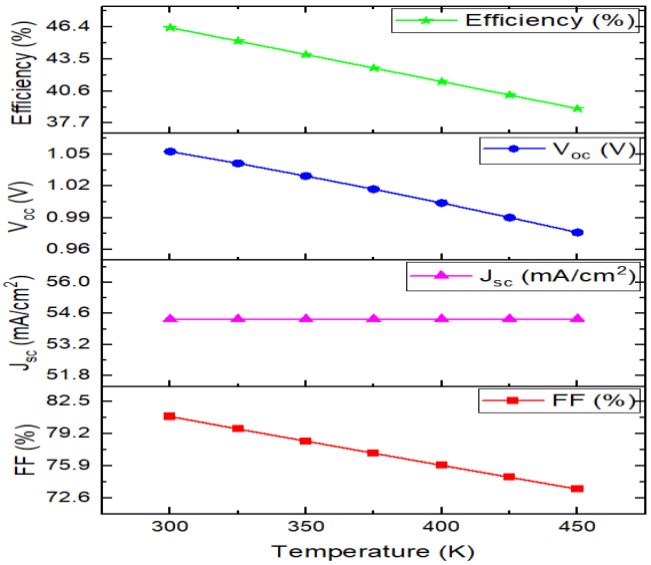

Fig. 8. Impact of operating temperature on BSF Layer

6. JV Curve Characteristics

JV (current density-voltage) curve visually depicts the solar cell's performance. Plotting the current density (J_{sc}) vs the voltage (V_{oc}) provides crucial information on the cell's open-circuit voltage, short-circuit current density, efficiency, and fill factor.

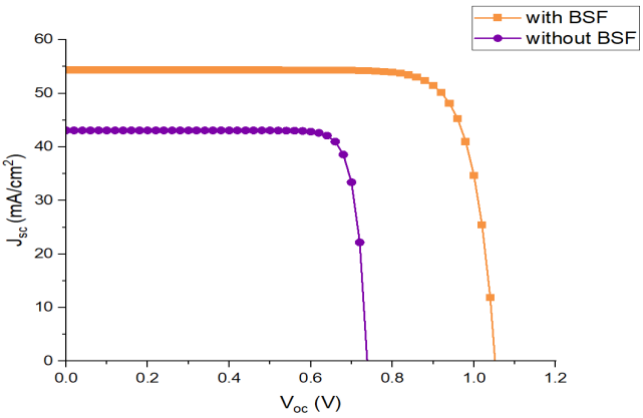

Fig. 9. Comparative study of J-V characteristics curve with and without BSF

J-V curve characteristics for the suggested cell shape are displayed in "Figure 9". The graph indicates that the suggested cell structure performs better with BSF than without BSF.

7. Quantum Efficiency

The capacity of a solar cell to convert photons of different wavelengths into electrical current is measured by its quantum effectiveness, or *QE*. The *QE* spectrum of a $CuSbSe_2$ solar cell shows the percentage of photons that are absorbed and changed into charge carriers (electrons or holes) as a function of wavelength. Effective photon absorption and conversion to electrical current are indicated by a high *QE*, whereas inefficient absorption or significant losses are indicated by a low *QE*.

QE (λ) = (Number of collected electron-hole pairs) / (Number of incident photons)

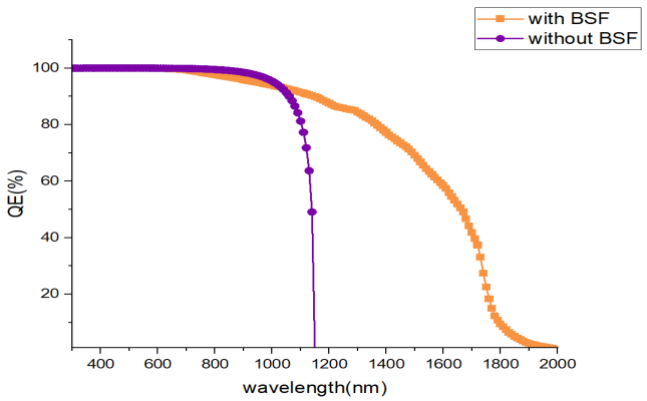

Fig. 10. Quantum Efficiency of $CuSbSe_2$ solar cell

Because most materials have a larger absorption coefficient at shorter wavelengths, "Figure 10" shows that the quantum efficiency approaches 100% for wavelengths less than 800 nm. This suggests that the material absorbs a higher percentage of photons with shorter wavelengths. Thus, additional electron-hole pairs are produced, raising the *QE*. The BSF layer, which also functions as the bottom absorber layer, absorbs photons with longer wavelengths using the TSA's two-step photo up conversion process. Furthermore, BSF layer increases the intrinsic potential of the $CuSbSe_2$/CGS contact, which increases the V_{oc}. As such, quantum efficiency for dual heterojunctions is toward longer wavelengths in comparison to single heterojunctions without a BSF layer.

Table 2. Comparative table presenting recent research with various device configurations

Cell Structure	V_{oc} (V)	J_{sc} (mA/cm^2)	FF (%)	PCE (%)	Cell Structure	Reference
$CuSbSe_2$/*n*-Zno/Al:Zno (Experimental)	0.34	18.84	47.34	3.04	Single	[14]
$CuSbSe_2$/*n*-Zno/Al:Zno (Experimental)	0.38	24.5	41	3.8	Single	[35]
$CuSbSe_2$/ZnS/ ITO	0.702 ± 0.008	36.97 ± 0.21	41.54 ± 1.38	10.79 ± 1.45	Single	[36]
n-ZnSe/*p*-$CuSbSe_2$/p^+-MoS_2 + *n*-ZnSe/*p*-$CdSe_2$/p^+-MoS_2	2.09	24.09	84.36	42.64	Tandem	[37]
n-ZnSe/*p*-$CuSbSe_2$	0.73	44.07	85.13	27.74	Single	[23]
n-ZnSe/*p*-$CuSbSe_2$/p^+-CGS	0.935	58.943	79.46	43.77	Dual Heterojunction	[23]
n-CdS/*p*-$CuSbSe_2$/Ni	0.738	43.08	85.23	27.12	Single	This work
n-CdS/*p*-$CuSbSe_2$/p^+-CGS/Ni	1.053	54.34	80.97	46.32	Dual Heterojunction	This work

8. Conclusion

CdS window layer and CGS BSF layer were used in the simulation to compare and optimize performance for $CuSbSe_2$ solar cell creation. Total efficiency of single cell n-CdS/ p-$CuSbSe_2$/Ni structure is 27.12 % with V_{oc}= 0.738 V, J_{sc} =43.08 mA/cm^2, and FF=85.23 %. Efficiency for dual heterojunction cell structure n-ZnSe/p-$CuSbSe_2$/p^+CGS/Ni is 46.32% with V_{oc}=1.053V, J_{sc}=54.34 mA/cm^2 & FF=80.97% and the Thermal stability is also assessed at each level, leading to computation of the temperature coefficient at the end which is (-0.042%/◦C). This study effort addresses the primary issues in solar cell research, including material preservation, efficiency booster, and thermal stability. Additionally, this research may lessen to the carbon footprint of energy production, promote sustainable manufacturing and disposal methods, and provide a clean and renewable energy source.

References

[1] A. M. Adekanmi, O. V. Mbelu, Y. B. Adediji and a. D. I. Yahya., "A review of current trends in thin film solar cell technologies," *International Journal of Energy and Power Engineering 17,* vol. 1, pp. 1-10, 2023.

[2] M. A. Green, Y. Hishikawa, E. D. Dunlop, D. H. Levi, J. Hohl-Ebinger and A. W. Ho-Baillie, "Solar cell efficiency tables (version 52)," *Prog Photovolt Res Appl,* vol. 26, p. 427–436, 2018.

[3] P. Jackson, R. Wuerz, D. Hariskos, E. Lotter, W. Witte and M. Powalla, "Effects of heavy alkali elements in Cu (In, Ga) Se2 solar cells with efficiencies up to 22.6%," *physica status solidi (RRL)–Rapid Research Letters,* vol. 10(8), pp. 583-586, 2016.

[4] F. Javed, "Impact of Temperature & Illumination for Improvement in Photovoltaic System Efficiency," *International Journal of Smart Grid - ijSmartGrid,* vol. 6(1), pp. 19-29, 2022.

[5] M. Dey, N. K. Das, M. Dey, S. F. U. Farhad, M. A. Matin and N. Amin, "Impact of Source to Substrate Distance on the Properties of Thermally Evaporated CdS Film," *International Journal of Renewable Energy Research (IJRER),* vol. 11(1), pp. 495-503, 2021.

[6] N. K. Das, S. F. U. Farhad, J. Chakaraborty, A. K. S. Gupta, M. Dey and M. Al-Mam, "Structural and optical properties of RF-sputtered CdTe thin films

grown on CdS: O/CdS bilayers," *International Journal of Renewable Energy Research*, vol. 10(1), pp. 293-302, 2020.

[7] S. A. Razi, N. K. Das, S. F. U. Farhad and M. A. M. Bhuiyan, "Influence of the CdCl2 solution concentration on the properties of CdTe thin films.," *International Journal of Renewable Energy Research (IJRER)*, vol. 10(2), pp. 1012-1020, 2020.

[8] E. M. K. I. Ahamed, N. K. Das, A. K. S. Gupta, M. N. I. Khan, M. A. Matin and N. Amin, "Structural and optical characterization of As-grown and annealed ZnxCd1-xS thin-films by CBD for solar cell applications," *International Journal of Renewable Energy Research*, vol. 10(3), pp. 1464-1474, 2020 Sep 23.

[9] D. Wang, W. Zhao, Y. Zhang and S. F. Liu, "Path towards high-efficient kesterite solar cells," *Journal of Energy Chemistry*, vol. 27, no. 4, pp. 1040-1053, 2018.

[10] B. Yang, D. J. Xue, M. Leng, J. Zhong, L. Wang, H. Song, Y. Zhou and J. Tang, "Hydrazine solution processed Sb2S3, Sb2Se3 and Sb2 (S1− xSex) 3 film: molecular precursor identification, film fabrication and band gap tuning," *Scientific reports 5*, vol. 1, p. 10978, 2015.

[11] S. Bhattacharjee, M. Hassan, N. K. Das and M. Dey, "Design and Optimization of Copper Antimony Sulfide Thin Film Solar Cell," *International Journal of Renewable Energy Research (IJRER)*, vol. 13(3), pp. 1398-1405, 2023 Sep 27.

[12] A. W. Welch, L. L. Baranowski, H. Peng, H. Hempel, R. Eichberger, T. Unold, S. Lany, C. Wolden and A. Zakutayev, "Trade-offs in thin film solar cells with layered chalcostibite photovoltaic absorbers," *Advanced energy materials* , vol. 7 (11), p. 1601935, 2017.

[13] D. J. Xue, B. Yang, Z. K. Yuan, G. Wang, X. Liu, Y. Zhou, L. Hu, D. Pan, S. Chen and J. Tang, "CuSbSe2 as a potential photovoltaic absorber material: studies from theory to experiment," *Advanced energy materials*, vol. 5(23), p. 1501203, 2015.

[14] C. Wang, B. Yang, R. Ding, W. Chen, R. Kondrotas, Y. Zhao, S. Lu, Z. Li and J. Tang, "Reactive close-spaced sublimation processed CuSbSe2 thin films and their photovoltaic application," *APL materials*, vol. 6(8), 2018.

[15] D. Tang, J. Yang, F. Liu, Y. Lai, J. Li and Y. Liu, "Growth and characterization of CuSbSe2 thin films prepared by electrodeposition," *Electrochimica acta*, vol. 76, pp. 480-486, 2012.

[16] H. Hsiang, C. Yang and J. Tu, "Characterization of CuSbSe2 crystallites synthesized using a hot injection method," *RSC advances*, vol. 6(101), pp. 99297-99305, 2016.

[17] D. Colombara, L. Peter, K. Rogers, J. Painter and S. Roncallo, "Formation of CuSbS2 and CuSbSe2 thin films via chalcogenisation of Sb–Cu metal precursors," *Thin Solid Films*, vol. 519(21), pp. 7438-7443, 2011.

[18] L. Wang, B. Yang, Z. Xia, M. Leng, Y. Zhou, D. Xue, J. Zhong, L. Gao, H. Song and J. Tang, "Synthesis and characterization of hydrazine solution processed Cu12Sb4S13 film," *Solar Energy Materials and Solar Cells*, vol. 144, pp. 33-39, 2016.

[19] B. Yang, Wang, C., Z. Yuan, S. Chen, Y. He, H. Song, R. Ding, Y. Zhao and J. Tang, "Hydrazine solution processed CuSbSe2: Temperature dependent phase and crystal orientation evolution.," *Solar energy materials and solar cells*, vol. 168, pp. 112-118, 2017.

[20] S. P. Bremner, M. Y. Levy and C. B. Honsberg, "Analysis of tandem solar cell efficiencies under AM1. 5G spectrum using a rapid flux calculation method," *Progress in photovoltaics: Research and Applications*, vol. 16(3), pp. 225-233, 2008.

[21] A. Kuddus, A. Bakar, M. Ismail and J. Hossain, "Design of a highly efficient CdTe-based dual-heterojunction solar cell with 44% predicted efficiency," *Solar Energy Volume*, vol. 221, pp. 488-501, 2021 June.

[22] A. Martí and A. Luque, "Three-terminal heterojunction bipolar transistor solar cell for high-efficiency photovoltaic conversion," *Nature communications*, vol. 6902, p. 6(1), 2015.

[23] B. Saha, B. Mondal, S. Mostaque, M. Hossain and J. Hossain, "Numerical modeling of CuSbSe2-based dual-heterojunction thin film solar cell with CGS back surface layer," *AIP Advances*, vol. 13(2), 2023.

[24] R. Bube, "Imperfection ionization energies in CdS-type materials by photoelectronic techniques," *Solid State Physics (Academic Press)*, vol. 11, pp. 223-260, 1960.

[25] S. Das and A. Beltran, "High Efficiency non-toxic CuSbS 2-based Heterojunction Solar Cell with TiO 2 Electron Transport Layer," in *IEEE 46th Photovoltaic Specialists Conference (PVSC) (pp. 1876-1879). IEEE*, Chicago, IL, USA, 2019.

[26] Y. H. Khattak, F. Baig, B. Marí, S. Beg, S. R. Gillani and T. Ahmed, "Effect of CdTe back surface field on the efficiency enhancement of a CGS based thin film solar cell," *Journal of Electronic Materials*, vol. 47(9), pp. 5183-5190, 2018.

[27] S. Ishizuka, "CuGaSe2 thin film solar cells: challenges for developing highly efficient wide-gap chalcopyrite photovoltaics.," *physica status solidi (a)*, vol. 216(15), p. 1800873, 2019.

[28] J. Song, S. Li, C. Huang, T. Anderson and O. Crisalle, "Modeling and simulation of a CuGaSe/sub 2//Cu(In/sub 1-x/,Ga/sub x/)Se/sub 2/ tandem solar cell," in *3rd World Conference onPhotovoltaic Energy Conversion, 2003. Proceedings of, Osaka, Japan, 2003, pp. 555-558 Vol.1.*, Osaka, Japan, 2003.

[29] O. Vigil-Galán, M. Courel, J. Andrade-Arvizu, Y. Sánchez, M. Espíndola-Rodríguez, E. Saucedo, D. Seuret-Jiménez and R. González, "Processing pathways of Cu2Zn (SnGe) Se4 based solar cells: The role of CdS buffer layer," *Materials Science in Semiconductor Processing*, , vol. 67, pp. 14-19, 2017.

[30] S. Ferrá-González, D. Berman-Mendoza, R. García-Gutiérrez, S. Castillo, R. Ramírez-Bon, B. Gnade and M. Quevedo-López, "Optical and structural properties of CdS thin films grown by chemical bath deposition doped with Ag by ion exchange," *Optik*, vol. 125(4), pp. 1533-1536, 2014.

[31] S. Butt, N. Shah, A. Nazir, Z. Ali and A. Maqsood, "Influence of film thickness and In-doping on physical properties of CdS thin films," *Journal of alloys and compounds*, vol. 587, pp. 582-587, 2014.

[32] A. Rmili, F. Ouachtari, A. Bouaoud, A. Louardi, T. Chtouki, B. Elidrissi and H. Erguig, "Structural, optical and electrical properties of Ni-doped CdS thin films prepared by spray pyrolysis.," *Journal of alloys and Compounds*, vol. 557, pp. 53-59, 2013.

[33] S. Ivanov, A. Piryatinski, J. Nanda, S. Tretiak, K. Zavadil, W. Wallace, D. Werder and V. Klimov, "Type-II core/shell CdS/ZnSe nanocrystals: synthesis, electronic structures, and spectroscopic properties," *Journal of the American Chemical Society*, , vol. 129(38), pp. 11708-11719, 2007.

[34] B. K. Mondal, S. K. Mostaque, M. A. Rashid, A. Kuddus, H. Shirai and a. J. Hossain, "Effect of CdS and In3Se4 BSF layers on the photovoltaic performance of PEDOT: PSS/n-Si solar cells: Simulation based on experimental data," *Superlattices and Microstructures* , vol. 152, p. 106853, 2021.

[35] S. Rampino, F. Pattini, M. Bronzoni, M. Mazzer, M. Sidoli, G. Spaggiari and E. Gilioli, "CuSbSe2 thin film solar cells with~ 4% conversion efficiency grown by low-temperature pulsed electron deposition," *Solar energy materials and solar cells*, vol. 185, pp. 86-96, 2018.

[36] P. Singh, S. Rai, P. Lohia and D. Dwivedi, "Comparative study of the CZTS, CuSbS2 and CuSbSe2 solar photovoltaic cell with an earth-abundant non-toxic buffer layer," *Solar Energy*, vol. 222, pp. 175-185, 2021.

[37] S. Shiddique, A. Abir, M. Hossain, M. Hossain and J. Hossain, "Design and optimization of CdSe-CuSbSe2-based double-junction two-terminal tandem solar cells with VOC> 2.0 V and PCE over 42%," no. arXiv preprint arXiv:2402.03853, 2024.